

Electronic Supplementary Information (ESI) for The UV Absorption Spectrum of the Simplest Criegee Intermediate CH₂OO

Wei-Lun Ting¹, Ying-Hsuan Chen¹, Wen Chao,^{1,2} Mica C. Smith,^{1,3} Jim Jr-Min Lin^{1,2,4*}

¹ Institute of Atomic and Molecular Sciences, Academia Sinica, Taipei, Taiwan

² Department of Chemistry, National Taiwan University, Taipei, Taiwan

³ Department of Chemistry, University of California at Berkeley, Berkeley, CA 94720, USA

⁴ Department of Applied Chemistry, National Chiao Tung University, Hsinchu, Taiwan

* Email: jimlin@gate.sinica.edu.tw

I. CH₂OO synthesis and transient absorption spectrometer

The Criegee intermediate CH₂OO was synthesized by the reaction of CH₂I with O₂; CH₂I was prepared by photodissociation of CH₂I₂. In the transient absorption experiment, CH₂I₂ vapor was carried with a controlled flow of N₂ or O₂. The mixing ratios of the reagent gases (CH₂I₂, N₂, O₂, SO₂) were controlled with mass flow controllers (Brooks Instruments, 5850E). They were mixed in a Teflon tube before entering the photolysis cell (750 mm long, 20 mm inner diameter). The linear flow velocity in the sample cell was adjusted to be faster than 0.8 m/s to allow refreshment of the sample gas between the photolysis laser pulses (~1 Hz repetition rate).

The setup of the transient absorption spectrometer has been described elsewhere.^{1,2} The output of a laser-driven plasma light source (Energetiq, EQ-99) was collimated by a parabolic mirror (Newport, 50329AL, f = 50.8 mm) before entering the sample tube. Another parabolic mirror (Newport, 50338AL, f = 101.6 mm) was used to focus the light into the slit of the intensified CCD (iCCD) spectrometer (Spectrometer: Andor SR303i; iCCD: Andor iStar DH320T-18F-E3). The wavelength scale of the spectrometer was calibrated with the emission spectrum of a mercury lamp. The photolysis laser beam (Coherent, CompExPro 205F, KrF 248 nm) was introduced into the cell by reflection from an ultrasteep long-pass edge filter (Semrock LP02-257RU-25), which also limited the probe wavelength to be longer than 260 nm.

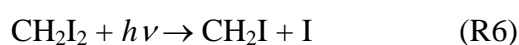
The delay time (kinetic time) is defined as the time from the photolysis laser pulse to the center of the detector gate (width = 1 μs). The reference spectrum is taken before the photolysis laser pulse. The delay time was scanned automatically at each photolysis pulse by using a program code of

Andor Basic. A typical delay time scan was repeated 60–200 times to achieve an adequate signal-to-noise ratio.

II. Subtraction of the absorbance of CH₂I₂ and IO

1. With SO₂ scavenging

Under our experimental conditions, we consider mainly the following reactions at the studied delay times (1–500 μs).



The number densities of O₂ (> 3×10¹⁷ cm⁻³) used were high enough to convert CH₂I to either CH₂OO or ICH₂OO within a few μs ($k_8 \sim 1 \times 10^{-12}$ cm³ sec⁻¹).^{3,4,5,6}

When adding SO₂ to the reaction system, CH₂OO is efficiently removed within a short period of time (see Figure 1c). As a result, the transient absorption spectra would mainly consist of the following contributions. (i) Depletion of CH₂I₂ and SO₂. (ii) Formation of ICH₂OO, SO₃, H₂CO, and IO.

We further analyze the spectra with the following guidelines. (1) The UV absorption cross sections of SO₃ and H₂CO are much smaller than those of CH₂OO (by 2 orders of magnitude in the wavelength region of interest). Therefore their contributions can be ignored. (2) The contribution of IO can be readily extracted by using the distinctive structures of the IO spectrum. (3) The yield of CH₂OO is assumed to be independent on [SO₂]. (4) In (R2), the amount of the reacted SO₂ molecules is the same as that of the reacted CH₂OO.

By taking the difference between the transient absorption spectra at low (zero) and high SO₂ concentrations (other conditions were kept the same), the difference spectra would contain mainly the contributions of CH₂OO and SO₂ with a 1:1 ratio, because the contributions of other absorbing

species like CH_2I_2 , ICH_2OO , etc. would not be affected by SO_2 and would be cancelled. Figure S1 shows the resulted spectra at three total pressures.

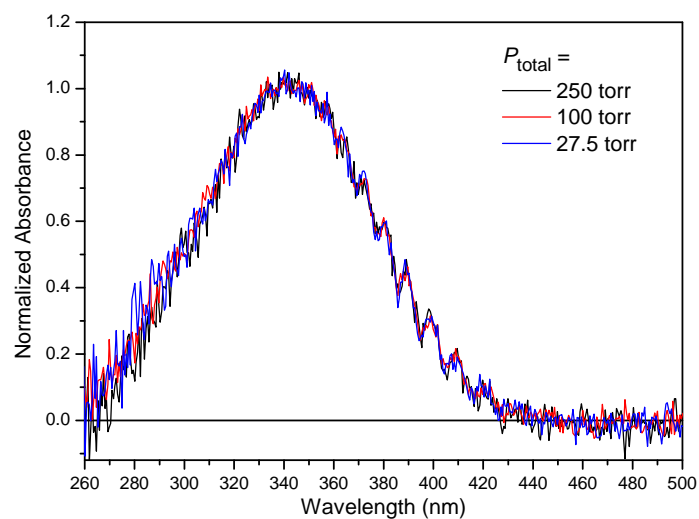


Figure S1. Height-normalized spectra of $\text{CH}_2\text{OO} + \text{SO}_2$ obtained with the SO_2 scavenging method at different cell pressures.

After we scaled the CH_2OO spectrum to the absolute cross section at 308.4 nm (see the main text), the contribution of SO_2 can be subtracted based on the known SO_2 cross sections. Figure S2 shows the scaled raw difference spectrum (the average spectrum of Figure 2b) and the effect of removing the SO_2 contribution.

After CH_2OO is fully consumed by SO_2 , the transient absorption spectrum would mostly consist of (i) depletion of CH_2I_2 and SO_2 and (ii) formation of ICH_2OO and IO . At low pressures, the yield of ICH_2OO is minor.³⁻⁶ After accounting for the amounts of ICH_2OO , IO and SO_2 as mentioned above, the amount of the photolyzed CH_2I_2 can be determined.

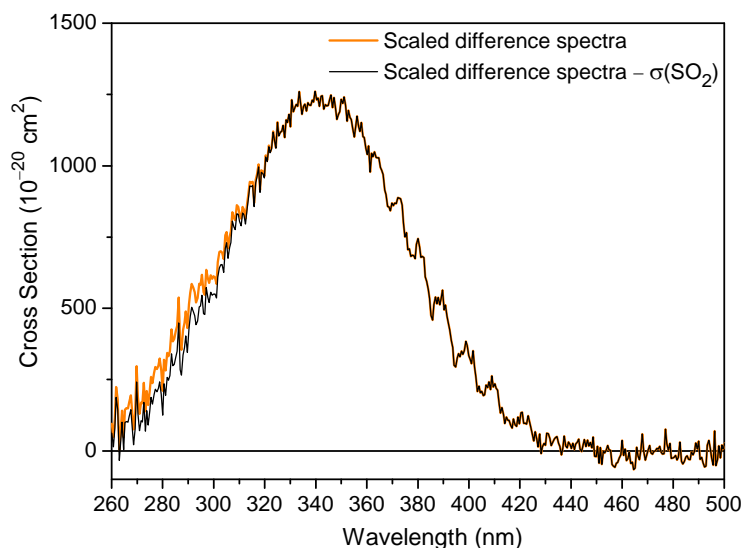
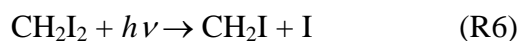


Figure S2. The thick orange line shows the average spectrum of Figure 2b ($P_{\text{total}} = 100$ torr) which has been scaled to the absolute cross section at 308.4 nm. The thin black line shows the net spectrum of CH_2OO after subtracting the SO_2 contribution (also shown in Figure 4).

2. Without adding SO_2

When SO_2 is absent, the main reactions to be considered are listed below.



At the low pressure limit, we may ignore the contribution of ICH_2OO .³⁻⁶ Similar to the case of adding SO_2 , the contribution of IO can be easily extracted. Then we need to determine the amount of the photolyzed CH_2I_2 , which can be obtained at longer delay times when CH_2OO is fully consumed by (R8) and (R9). The amount of the photolyzed CH_2I_2 determined in this way is similar (within 10%) to that determined by adding SO_2 , indicating the validity of these two approaches.

A small fraction of CH₂ might be produced through the photolysis of CH₂I (CH₂I + *hν* → CH₂ + I). We have checked the transient absorption spectra at various laser pulse energies from 30 to 100 mJ/pulse. A small decrease in the yield of CH₂I was observed at high laser power. However, no significant difference can be found in the deduced spectrum of CH₂OO, indicating CH₂ and its subsequent products absorb rather weakly in this spectral range.

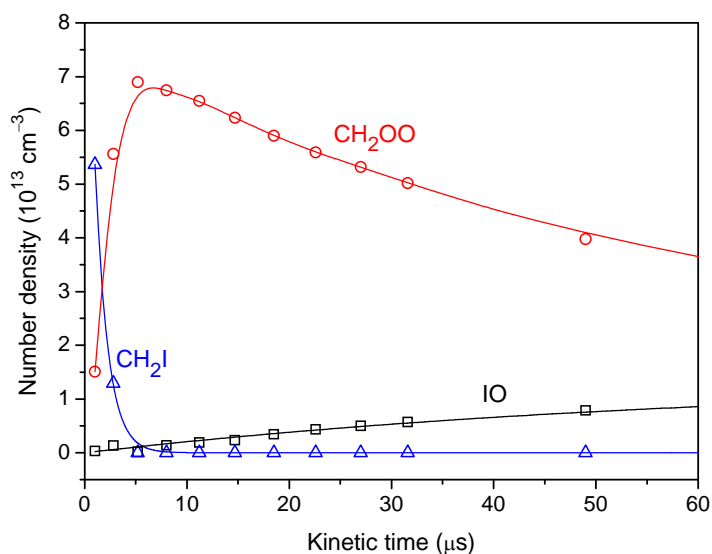


Figure S3. Example of the number density profiles of CH₂I (triangle), CH₂OO (circle) and IO (square) in the photolysis reaction system of CH₂I₂/O₂. The lines are only to guide the eye, not kinetic fit. The [CH₂I₂]₀, [O₂]₀ and the total number density *n*_{total} (N₂ balance) were 1.1×10¹⁵, 6.1×10¹⁷ and 7.2×10¹⁷ cm⁻³, respectively. The photolyzed [CH₂I₂] was 1.0×10¹⁴ cm⁻³. The decay of CH₂I and the formation of CH₂OO are well correlated. The time constants of these two processes are about 1 μs, which is consistent with the pseudo-first-order rate coefficient $k_7' = k_7[\text{O}_2] = (1.6 \times 10^{-12} \text{ cm}^3 \text{ s}^{-1})(6.1 \times 10^{17} \text{ cm}^{-3}) = 9.8 \times 10^5 \text{ s}^{-1}$. The value of *k*₇ is adapted from the average value of Refs. 3 and 4. After the rapid formation of CH₂OO, the self-reaction of CH₂OO (R9) and the reaction of CH₂OO with I atoms (R8) caused decay of CH₂OO and formation of IO.

III. Estimate the absolute absorption cross section in the bulk condition

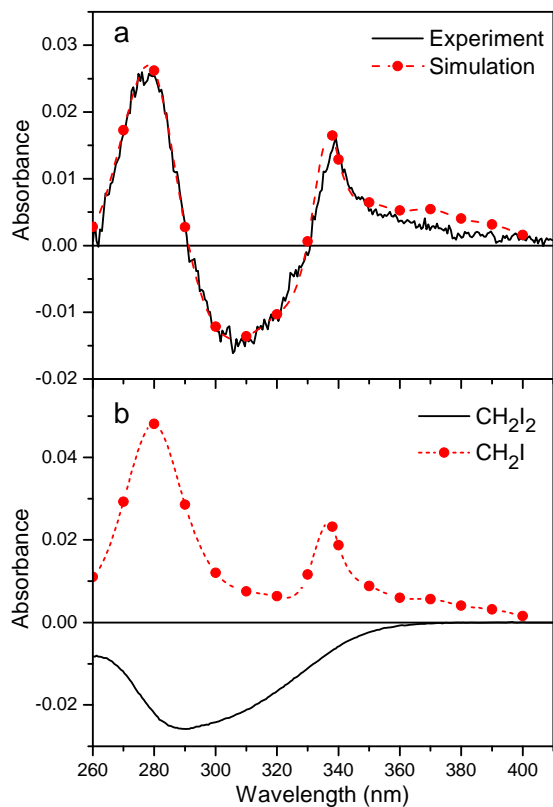


Figure S4. (a) Example of our transient absorption spectra when O_2 was absent (buffer gas = N_2). The spectrum can be simulated with the contributions from CH_2I (formation) and CH_2I_2 (depletion). (b) Published spectra^{7,8} of CH_2I_2 and CH_2I scaled to fit the experimental spectrum in (a).

Table S1. Estimation of the number density and absorption cross section of CH₂OO

P (torr)	n (cm ⁻³)	[O ₂] (cm ⁻³)	[CH ₂ I] ₀ (cm ⁻³) ^a	$\Phi_{\text{CH}_2\text{OO}}$	[CH ₂ OO] ₀ (cm ⁻³)	$A_{\text{CH}_2\text{OO}}$	$\sigma_{\text{CH}_2\text{OO}}$ (cm ²) ^d
			2.78x10 ¹³	0.541 ^b	1.51x10 ¹³	0.0130 ^c	1.34x10 ⁻¹⁷
121	3.96x10 ¹⁸	8.14x10 ¹⁷	6.25x10 ¹³	0.541	3.39x10 ¹³	0.0309	1.43x10 ⁻¹⁷
			1.14x10 ¹⁴	0.541	6.14x10 ¹³	0.0513	1.31x10 ⁻¹⁷
10.6	3.48x10 ¹⁷	3.20x10 ¹⁷	5.11x10 ¹³	0.858	4.38x10 ¹³	0.0366	1.31x10 ⁻¹⁷
			7.97x10 ¹³	0.858	6.83x10 ¹³	0.0523	1.20x10 ⁻¹⁷
Selected Estimation: (1.26±0.26)x10 ⁻¹⁷							

Where P is the total pressure, n is the total number density.

^a Estimated from the observed absorbance and the published cross section of Ref. 8. Typical [CH₂I]₀ was more than 10 times of [CH₂I]₀.

^b The quantum yield of CH₂I + O₂ → CH₂OO + I (R7a), estimated from the pressure dependent yield of Ref. 4, $\Phi_{\text{CH}_2\text{OO}} = (1.1 + 1.9 \times 10^{-19} n)^{-1}$. The quoted error bar is ±20% or more (pressure dependent). The quantum yields of Ref. 3 are within the range of the error bar.

^c Observed maximum peak absorbance among the data at different delay times.

^d The peak value at 340 nm. We choose the low-pressure (10.6 torr) result as our selected estimation because the error in $\Phi_{\text{CH}_2\text{OO}}$ is smaller at lower pressures. The overall error bar is estimated to be ±20%, mostly due to the error bar of $\Phi_{\text{CH}_2\text{OO}}$.^{3,4}

IV. Absolute photo-depletion cross section with molecular beam

1. Experimental Setup

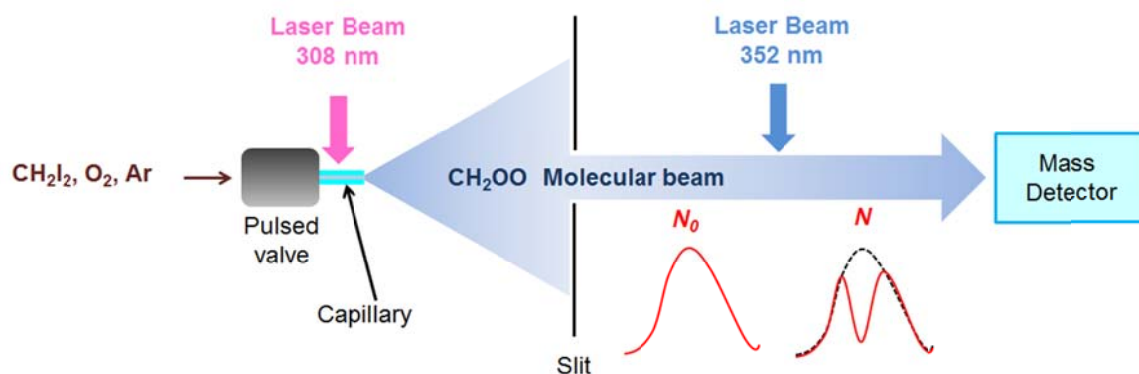


Figure S5. Schematic of the molecular beam experiment.

As illustrated in Figure S5, we made a molecular beam (similar to Ref. 9) containing CH₂OO and only measured the number of CH₂OO molecules with a mass spectrometric detector before and after laser irradiation. After absorbing a photon, the excited CH₂OO will dissociate in a time scale much shorter than the transient time to the detector (~ 1 millisecond); thus, the number of CH₂OO radicals reaching the detector is reduced. The probability of the photodissociation is proportional to the absorption cross section σ , dissociation quantum yield ϕ and the laser fluence I . For a group of molecules that dissociate very fast (≤ 1 ps) after absorbing a photon, other slower stabilization processes like emitting another photon (which requires more than 1 ns) cannot compete with dissociation at all, leading to 100% dissociation ($\phi = 1$). This group of fast dissociating molecules includes CH₂OO and our reference molecule like CH₂I₂. As the upper limit of ϕ is 1, the error bar of ϕ is negligible in our studied cases.

The depletion laser (25 Hz) was fired at every other molecular beam pulses (50 Hz), such that half the molecular beam pulses did not interact with the depletion laser and served as the reference signal in the photodepletion measurement. For the depletion experiment at 308.4 nm, the laser wavelength used to photolyze CH₂I₂ was 351.8 nm. For the depletion experiment at 351.8 nm, the laser wavelength used to photolyze CH₂I₂ was 308.4 nm.

2. Results at 351.8 nm

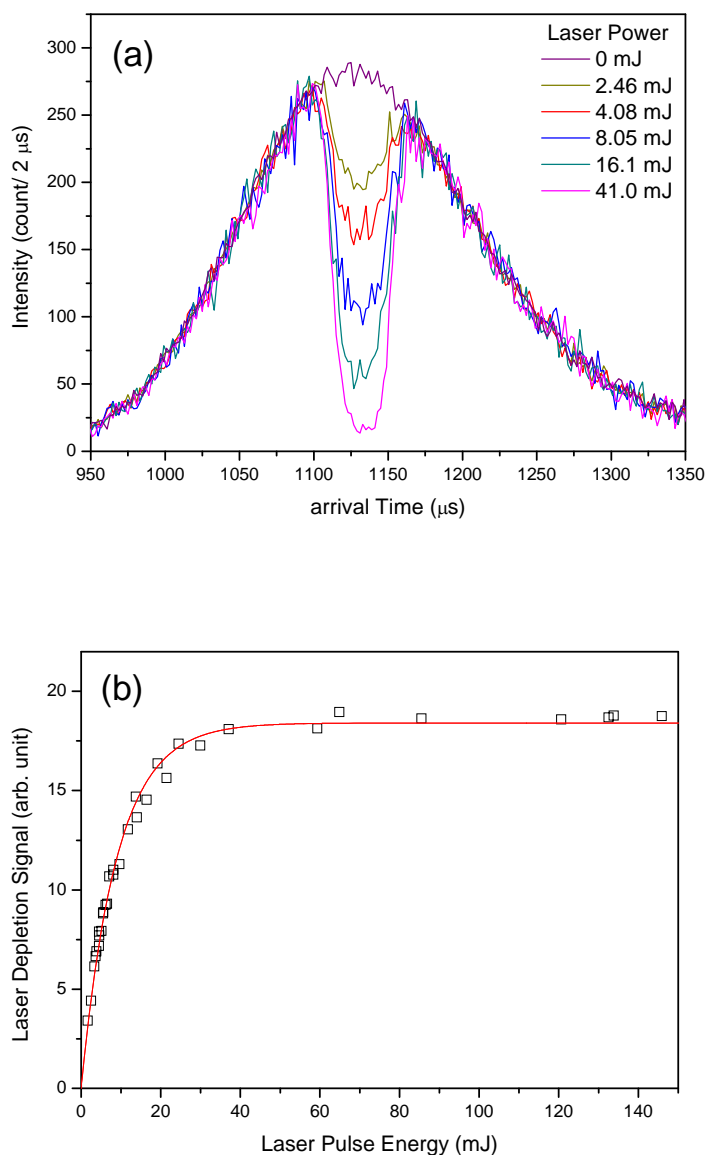


Figure S6. (a) Arrival time profiles of CH_2OO molecular beam upon laser irradiation at various laser fluences at 351.8 nm. The parent ion of CH_2OO was detected at $m/z = 46$ amu. (b) Saturation curve for the laser depletion of CH_2OO at 351.8 nm. The x-axis is the laser pulse energy which is linear to the laser fluence. The y-axis is the integral signal of the laser depletion percentage. The line is the fit of Equation 1. The nice fit also indicates the laser depletion experiment is a single-photon process.

3. List of the cross section ratio from each photodepletion measurement.

TableS2.

Wavelength (nm)	308.4	351.8
$\frac{\sigma\phi(\text{CH}_2\text{OO})}{\sigma\phi(\text{CH}_2\text{I}_2)}$	2.55	46.5
	2.41	49.7
	2.74	47.3
	2.41	44.2
	2.48	46.2
	2.55	51.5
	–	46.5
	Average	2.52
Standard deviation	0.14	2.6

V. Table of the cross sections

Table S3. The UV absorption cross sections of CH₂OO (using the SO₂ scavenging method).

Wavelength λ is in nm and absorption cross section σ is in 10^{-20} cm². The estimated relative error is about 12% for 280–290 nm, 9% for 290–300 nm, 7% for 300–310 nm, <5% for 310–484 nm.

λ	σ										
280.0	164	297.1	509	314.1	865	331.2	1176	348.2	1157	365.3	1004
280.6	217	297.7	512	314.7	932	331.8	1162	348.8	1192	365.8	962
281.2	192	298.2	570	315.3	921	332.3	1184	349.4	1196	366.4	954
281.7	267	298.8	604	315.8	878	332.9	1214	349.9	1200	367.0	890
282.3	218	299.4	562	316.4	958	333.5	1208	350.5	1194	367.5	881
282.9	297	299.9	561	317.0	928	334.0	1213	351.1	1210	368.1	895
283.4	292	300.5	585	317.5	955	334.6	1199	351.6	1183	368.7	834
284.0	216	301.1	542	318.1	941	335.2	1205	352.2	1165	369.2	845
284.6	290	301.6	601	318.7	966	335.7	1176	352.8	1134	369.8	844
285.1	312	302.2	596	319.3	956	336.3	1182	353.3	1163	370.4	863
285.7	272	302.8	637	319.8	973	336.9	1207	353.9	1145	370.9	879
286.3	383	303.3	629	320.4	974	337.4	1183	354.5	1117	371.5	855
286.8	350	303.9	669	321.0	992	338.0	1225	355.0	1126	372.1	885
287.4	320	304.5	651	321.5	1041	338.6	1221	355.6	1123	372.7	873
288.0	329	305.0	672	322.1	1083	339.1	1227	356.2	1127	373.2	854
288.6	332	305.6	636	322.7	1073	339.7	1241	356.8	1138	373.8	826
289.1	417	306.2	702	323.2	1080	340.3	1240	357.3	1143	374.4	783
289.7	376	306.7	706	323.8	1046	340.8	1221	357.9	1133	374.9	767
290.3	365	307.3	742	324.4	1066	341.4	1230	358.5	1116	375.5	751
290.8	403	307.9	759	324.9	1082	342.0	1238	359.0	1090	376.1	721
291.4	441	308.5	734	325.5	1081	342.6	1208	359.6	1084	376.6	684
292.0	420	309.0	730	326.1	1098	343.1	1216	360.2	1033	377.2	698
292.5	416	309.6	793	326.6	1088	343.7	1197	360.7	1040	377.8	676
293.1	473	310.2	779	327.2	1109	344.3	1220	361.3	976	378.3	686
293.7	476	310.7	781	327.8	1127	344.8	1208	361.9	1020	378.9	686
294.2	425	311.3	784	328.3	1149	345.4	1224	362.4	1033	379.5	707
294.8	459	311.9	820	328.9	1125	346.0	1245	363.0	1020	380.0	728
295.4	503	312.4	835	329.5	1134	346.5	1187	363.6	1002	380.6	716
295.9	517	313.0	802	330.1	1130	347.1	1216	364.1	1026	381.2	697
296.5	511	313.6	878	330.6	1190	347.7	1196	364.7	1012	381.7	683

λ	σ										
382.3	656	399.3	374	416.3	67	433.4	38	450.4	-3	467.4	-21
382.9	644	399.9	344	416.9	99	433.9	23	450.9	-14	467.9	6
383.4	564	400.5	336	417.5	107	434.5	56	451.5	0	468.5	-20
384.0	576	401.0	314	418.0	71	435.1	39	452.1	-15	469.1	4
384.6	546	401.6	348	418.6	90	435.6	13	452.6	-3	469.6	-25
385.1	477	402.2	282	419.2	117	436.2	1	453.2	-8	470.2	5
385.7	463	402.7	239	419.8	123	436.8	27	453.8	-15	470.8	-13
386.3	476	403.3	207	420.3	117	437.3	27	454.3	-3	471.3	-25
386.8	501	403.9	197	420.9	115	437.9	42	454.9	0	471.9	8
387.4	501	404.4	188	421.5	91	438.5	5	455.5	-1	472.5	-2
388.0	541	405.0	190	422.0	86	439.0	17	456.0	-13	473.0	-25
388.5	533	405.6	177	422.6	126	439.6	-14	456.6	-19	473.6	19
389.1	559	406.1	193	423.2	81	440.2	-6	457.2	-49	474.2	4
389.7	550	406.7	223	423.7	85	440.7	13	457.7	-34	474.7	-2
390.2	512	407.3	222	424.3	54	441.3	11	458.3	-35	475.3	7
390.8	500	407.8	223	424.9	44	441.9	15	458.9	-2	475.9	7
391.4	463	408.4	227	425.4	55	442.4	-16	459.4	23	476.4	-43
392.0	422	409.0	237	426.0	43	443.0	-13	460.0	21	477.0	-38
392.5	392	409.5	241	426.6	22	443.6	-13	460.6	-13	477.6	-12
393.1	398	410.1	226	427.1	6	444.1	6	461.1	10	478.1	-15
393.7	364	410.7	211	427.7	6	444.7	29	461.7	-7	478.7	-38
394.2	315	411.2	210	428.3	4	445.3	31	462.3	-17	479.3	-28
394.8	297	411.8	140	428.8	5	445.8	8	462.8	-16	479.8	-13
395.4	296	412.4	139	429.4	42	446.4	-18	463.4	-26	480.4	16
395.9	338	412.9	147	430.0	53	447.0	-1	464.0	-31	480.9	-12
396.5	334	413.5	138	430.5	47	447.5	29	464.5	-29	481.5	-28
397.1	357	414.1	117	431.1	33	448.1	3	465.1	-47	482.1	1
397.6	365	414.6	105	431.7	30	448.7	20	465.7	-23	482.6	20
398.2	377	415.2	116	432.2	26	449.2	-14	466.2	-24	483.2	-29
398.8	382	415.8	99	432.8	44	449.8	2	466.8	-54	483.8	-15

References:

- ¹ M.-N. Su and J. J. Lin, *Rev. Sci. Instrum.* 2013, 84 , 086106.
- ² Man-Nung Su and Jim Jr-Min Lin, *GSTF Journal of Chemical Sciences (JChem)* (ISSN: 2339-5060) 2013, 1, 52–57. (DOI: 10.5176/2339-5060_1.1.6)
- ³ H. Huang, A. J. Eskola and C. A. Taatjes, *J. Phys. Chem. Lett.*, 2012, 3, 3399–3403; H. Huang, B. Rotavera, A. J. Eskola and C. A. Taatjes, *J. Phys. Chem. Lett.*, 2013, 4, 3824.
- ⁴ D. Stone, M. Blitz, L. Daubney, T. Ingham and P. Seakins, *Phys. Chem. Chem. Phys.*, 2013, 15, 19119-19124.
- ⁵ D. Stone, M. Blitz, L. Daubney, N. U. M. Howesa and P. Seakins, *Phys. Chem. Chem. Phys.* 2014, DOI: 10.1039/c3cp54391a.
- ⁶ O. Welz, J. D. Savee, D. L. Osborn, S. S. Vasu, C. J. Percival, D. E. Shallcross and C. A. Taatjes, *Science*, 2012, 335, 204–207.
- ⁷ S.P. Sander, J. Abbatt, J. R. Barker, J. B. Burkholder, R. R. Friedl, D. M. Golden, R. E. Huie, C. E. Kolb, M. J. Kurylo, G. K. Moortgat, V. L. Orkin and P. H. Wine "Chemical Kinetics and Photochemical Data for Use in Atmospheric Studies, Evaluation Number 17", JPL Publication 10-6, Jet Propulsion Laboratory, Pasadena, 2011. <http://jpldataeval.jpl.nasa.gov>
- ⁸ J. Sehested, T. Ellermann, and O.J. Nielsen, *Int. J. Chem. Kinet.* 1994, 26, 259-272.
- ⁹ J. M. Beames, F. Liu, L. Lu and M. I. Lester, *J. Am. Chem. Soc.*, 2012, 134, 20045–20048.